

Glauber Monte-Carlo Study of 200 GeV U+U Collisions

Christopher E. Flores
University of California, Davis REU 2009
Advisers: Daniel Cebra, Manuel Calderon, Jim Draper
REU Director: Rena Zieve

Collisions of deformed Uranium nuclei are studied using Glauber Monte-Carlo simulations in an effort to elucidate the effects of the non-symmetric rotations of prolate spheroid nucleus geometry and impact parameter. The nucleon density distribution is given by a three parameter Woods-Saxon density function and a Glauber Model is used in a Monte-Carlo simulation. The number of participant nucleons and number of nucleon-nucleon collisions is determined and compared to the results found for Gold using the same model. A comparison of gold and uranium collisions shows that tip to tip U+U collisions increase energy density by 35% while body to body collisions decrease energy density by 10%. It is also shown that a cut on the top 5% of the charged multiplicity density per unit transverse area results in no significant increase or decrease in collision energy density. Finally, plots of predicted Upsilon production values show expected Upsilon production of collisions at various impact parameters and full overlap orientations.

I. INTRODUCTION and MOTIVATION

Current experiments in high energy heavy ion collisions are concerned with studying the properties of the quark-gluon plasma (QGP) theorized to have existed in the fractions of a second after the big bang. Studies of this kind are accomplished by accelerating nuclei to near the speed of light and colliding them inside detectors sensitive enough to collect information about the particles emanating from the collision point. Such collisions are occurring at the Relativistic Heavy Ion Collider (RHIC) at Brookhaven National Laboratory and will occur at the Large Hadron Collider (LHC) at CERN when it becomes operational.

In general, a study of QGP at high energies will yield insights about our infant universe and further our understanding of phenomena at high energies. However, a property of QGP particularly interesting at present is the possibility that it could act as an ideal fluid with no viscosity. Center of mass energy of 200 GeV Au+Au collisions at RHIC have produced results suggesting that at such energies strongly interacting matter exists in the QGP phase. [1,7-10] A comparison of the flow quantities measured in these collisions with quantities predicted by ideal fluid calculations implies that 200 GeV central Au+Au collisions have just reached sufficiently high energy densities in small enough space-time volumes to exhibit ideal fluid like behavior. [2] As a test for ideal fluidity it would be useful to increase the energy density to see whether the flow quantity continues to increase or whether it peaks at the value for an ideal fluid.

The properties of QGP are inferred from studies concerning the particles emanating from the collision point of two nuclei. These particles carry with them information about the QGP in the form of charge, energy, and momentum. However, these particles can, and often do, interact with one another prior to reaching the detector. Since the probability

of interaction and mass are inversely related studies of high mass particles are most useful.

The bottom quark, a heavy quark with mass 4.2 GeV, is often studied at these energy levels. Since their mass precludes them from existing at all but the highest of energies these heavy quarks are necessarily studied during heavy ion collisions. The bottom quark is the lighter of the two third generation quarks and because studies of CP violation require all three quark generations the bottom quark is the easiest avenue to studying CP violation. The bottom quark is also interesting because it is a decay product of the top quark and is a possible decay particle of the Higgs Boson. These properties aside, the bottom quark is examined in QGP studies because its massive nature prevents it from interacting with other particles as it transverses the reaction plane. Thus, it can be used as a probe to study QGP properties.

Since quarks are unable to exist independently the bottom quark must be studied as constituents of a hadron such as the Upsilon meson (b,anti-b). However, the same property of the b quark which allows it to be useful in QGP studies also prevents it from being easily made. The more massive a particle the less likely it will be produced from an ion collision. Particle production rate increases with the energy density of the heavy ion collision. Thus, an increase in energy density results in an increase in particle production.

There exist two ways to increase the energy density of nuclei collisions. First, the machine can be upgraded with more powerful magnets and RF cavities to produce a more energetic beam and therefore higher center of mass collision energies. This method, while effective, proves to be difficult to achieve due to the price of components and construction time. A second possibility is that deformed nuclei can be used for collisions. When the long axes of the nuclei are oriented along the beam (Tip to Tip) the nucleon density per unit transverse area is greater than any other orientation. This leads to a higher probability of nucleon-nucleon interaction and therefore higher N_{part} and N_{coll} counts. This second method is

by far the most economical as it amounts to an upgrade for the machine without having to replace or improve any existing hardware.

It is clear then that if colliding deformed nuclei such as uranium increase the energy density of collisions in the tip to tip configuration, such collisions will be advantageous for both studies of QGP as an ideal fluid and particle studies such as those pertaining to the Upsilon meson. Taking into consideration the effects of the deformation characteristics of prolate spheroid geometry the present study aims to accomplish three goals: 1) examine the distribution of the five collision parameters; 2) show the affect of the prolate spheroid uranium geometry on collision energy density; and 3) make a prediction about Upsilon production from U+U collisions. A Monte-Carlo method is used with the Glauber Model and Woods-Saxon nucleon distribution to calculate the number of participating nucleons per U+U collision (N_{part}) and the number of nucleon-nucleon collisions per U+U collision (N_{coll}). This information is then used to accomplish the three goals.

The paper is organized in the following way: in Section II the model used for the study is developed and discussed, in Section III the results produced by the model for both gold and uranium are presented and discussed, and a brief summary and conclusion of the finding is presented in Section IV.

II. MODEL DEVELOPMENT

The Glauber Model is used as the basis of the model developed in this study. In a collision of two nuclei a nucleon from one nucleus can be thought of as sphere with finite radius “tunneling” through the other nucleus. In essence the nucleon cuts out a cylindrical path through the target nucleus. The number of nucleons within the target nucleus and with any part of their volume inside the cylinder are considered to have collided with the incident nucleon. In this way the number of nucleon-nucleon collisions can be counted for each nucleon of a nucleus. The total number of nucleon-nucleon collisions, N_{coll} , is the sum of all the nucleon-nucleon collisions counted for each incident nucleon. When N_{coll} is at least one that nucleon is considered to have participated in heavy ion collision. The total number of participating nucleons, N_{part} , is simply the sum of all participating nucleons in each nucleus.

The model development began with studying the collision geometry of nuclei. Au+Au collisions are modeled as collisions of two spheres. Because spheres are symmetric for all rotations Au+Au collisions have only one degree of freedom per collision, the impact parameter, b . This symmetry and the resulting one degree of freedom means that number of particles produced from a collision closely correlates solely with impact parameter. It follows that the centrality of a collision can be inferred from the multiplicity of the collision.

The collision geometry of U+U collisions is not as straight forward. As determined from experiments using gamma spectra Uranium nuclei are modeled as prolate spheroids. As

such they are only symmetric for rotations about their major axis. This results in a total of five degrees of freedom for each collision. The coordinate system used defines the beam direction to be along the z axis, the vertical direction to be the x axis, and the horizontal direction to be the y axis. A rotation in the zx plane and is represented with the polar angle, ϕ , and a rotation in the xy plane is represented by the azimuthal angle, θ . [Figure 2] The five degrees of freedom are therefore θ_1 and ϕ_1 for nucleus one, θ_2 and ϕ_2 for nucleus two, and b . A tip to tip collision occurs when $\theta_1=\theta_2=\phi_1=\phi_2=b=0$ and a broadside to broadside collision occurs when $\theta_1=\theta_2=\phi_1=\phi_2=\pi/2$ and $b=0$ or $\theta_1=\theta_2=b=0$ and $\phi_1=\phi_2=\pi/2$.

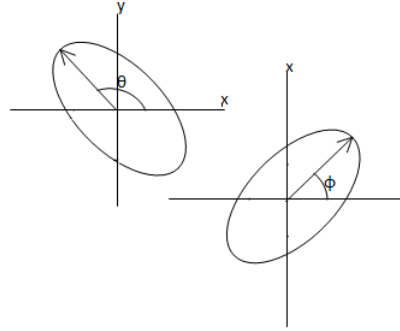


[Figure 2]: Illustration of spheroid rotations about each of the axis perpendicular the beam the beam direction, z.

The fact that U+U collisions have five degrees of freedom is a major complication for collision analysis. The number of particles emanating from a collision point is no longer directly dependent only on the impact parameter. Instead, the multiplicity is dependent on all five of the collision orientation parameters. Hence, one of the goals of this project is to determine how each of the collision parameters affects N_{part} and N_{coll} .

With an understanding of the collision geometry the model development phase could now proceeds to simulate nuclei collisions as the intersection of two “hard” objects. Each nucleus could be conceptualized as a prolate spheroid or sphere with sharp edges and a uniform nucleon distribution. Although N_{part} and N_{coll} can be calculated with this elementary model the uniform nucleon distribution used here is not consistent with the observed properties of the nucleus. In reality nuclei do not have sharp edges and the nucleon distribution follows that of Woods-Saxon distribution.

The Woods-Saxon Distribution was experimentally determined by electron scattering off various nuclei and is a common way of modeling the distribution of nucleons in the nucleus. The three parameter Woods-Saxon distribution suggests that there is a central nucleon density suppression to minimize the columbic potential, a maximum nucleon density radius, and then a fall off to zero density at infinite radius. The form of the deformed three parameter Woods-Saxon distribution as used in this study is

$$\rho(r, \theta) = \rho_0 \left(\frac{1 + \omega \left(\frac{r}{c} \right)^2}{1 + e^x} \right), \quad r < c, \quad (1) [4]$$

$$= \rho_0 \left(\frac{1+\omega}{1+e^x} \right), r \geq c$$

$$\text{where } x = \frac{r-c(1+\beta_{20}Y_{20}+\beta_{40}Y_{40})}{a(1+\beta_{20}Y_{20}+\beta_{40}Y_{40})}$$

The angle θ is the angle between the symmetry axis of the nucleus and the radius vector. The following constants were used for Gold and Uranium:

	ρ_0	ω	a	c	β_{20}	β_{40}
Au[11]	.169	0	.535	6.38	0	0
U[4]	.127	.5	.5	6.8	.254	.052

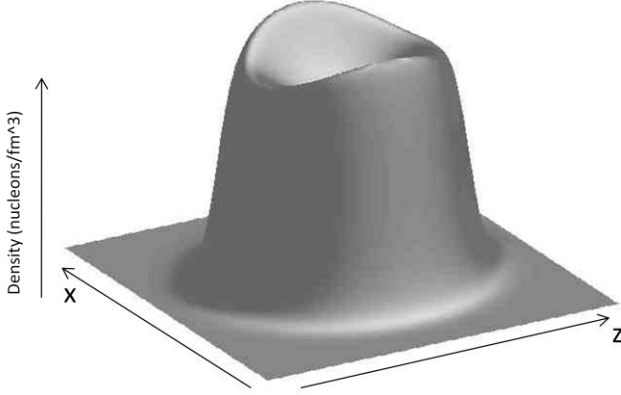


[Figure 3] Woods-Saxon Distribution in the x,z plane showing central nucleon suppression and the prolate geometry of the Uranium Nucleus.

Once the nucleons have been distributed in the nucleus according to a realistic nucleon distribution such as the Woods-Saxon all the necessary requirements for an analytical simulation are present. The analytic simulation begins with randomly generating the five collision orientation parameters. Each is distributed appropriately in phase space with θ ranging from zero to 2π and ϕ ranging from 0 to $\pi/2$. The collision geometry for each event is then found by scanning the incident nucleus in xyz and finding the largest ellipse or circle formed in the transverse (xy) plane. This transverse shape acts as a two dimensional constraint on which base the calculation of N_{part} and N_{coll} . The requirements for any given xyz location to be considered as contributing to N_{part} and N_{coll} are that it must be within the three dimensional volume of the target nucleus and within the two dimensional area of the transverse ellipse. If these requirements are met the density is found at each xyz location in each nucleus with the Woods-Saxon density distribution and N_{part} and N_{coll} are computed.

To compute N_{part} and N_{coll} the nuclei must be first collapsed into the transverse plane with a nuclear "Thickness" function. The thickness function is defined as the integral of the nuclear density of the longitudinal dimension (z axis) and takes the form [11]

$$T(b) = \int \rho(b, z) dz. \quad (2)$$

Here, b is the impact parameter and $\rho(b, z)$ is the density at a point (b,z) and a constant (x,y) using the Woods-Saxon density distribution. Hence the thickness function is at its maximum at the (x,y) with longest longitudinal distance (center of nucleus) and at its minimum at an (x,y) with the smallest longitudinal distance (edge of nucleus). The thickness function is commonly referred to as areal density.

Once a thickness has been computed for a given (x,y) for both nuclei, T_A and T_B , N_{part} and N_{coll} can be computed with the functions [11]

$$N_{part} = \iint T_A(1 - e^{-\sigma T_B}) + T_B(1 - e^{-\sigma T_A}) dx dy \quad (3)$$

$$N_{coll} = \sigma \int T_A T_B dx dy \quad (4)$$

where σ is the inelastic cross section of nucleon-nucleon interaction, 42mb.

The Monte-Carlo simulation begins with randomly generating the five collision orientation parameters just as was done in the analytic simulation. The rotated nuclei are then filled with 238 nucleons each. This is accomplished by generating random x,y,z coordinates and a Woods-Saxon variable for each nucleon. The Woods-Saxon density is then computed for the x,y,z location and if the Woods-Saxon variable is less than the computed density the generated nucleon location is accepted. Once both nuclei have been filled the transverse distance between each nucleon in the incident nucleus and each nucleon in the target matrix is computed. If the distance between two nucleons is less than 2 times the radius of a nucleon the nucleons are said to have collided and a count is added to the N_{coll} . The radius of the nucleon can be calculated from the inelastic cross section of the nucleon-nucleon interaction by $42\text{mb} = 4.2\text{fm} = \pi r^2$ where r is the radius of the smallest circle in which two touching but not overlapping nucleons can be inscribed. Thus $r/2 = r_{nucleon}$. N_{coll} is computed by summing the number of collisions each nucleon undergoes and N_{part} is computed by counting the number of nucleons having undergone at least one collision.

III. RESULTS AND DISCUSSION

Having now computed N_{part} and N_{coll} using the analytic and Monte-Carlo methods for both Gold and Uranium comparisons can be made between the two nuclei. First, the average results for N_{part} and N_{coll} for each of the simulations are shown. Second, it is shown how the five degrees of freedom of a U+U collision affect N_{part} and N_{coll} . Third, the energy density of a U+U collision is computed for the tip to tip and body to body configuration. These are then compared to central Au+Au collisions. Finally, the expected number of Upsilon's from U+U collisions is computed, discussed, and compared to the computed values of Upsilon production for Gold.

It should be noted that the analytic simulation suffered from an error resulting in an increase in events with high N_{part} and N_{coll} . [Figure A7, A9] While this issue is currently being

addressed, the results for the analytic simulation and analysis are included here only for completeness. Additionally, anomalous features of the Monte-Carlo simulation are also being studied.

N_{part} and N_{coll}

The following tables show the results of N_{part} and N_{coll} for both the analytic and Monte-Carlo simulations. Because the Uranium nucleus contains more nucleons it is expected that the numbers for N_{part} and N_{coll} will be larger for Uranium than Gold. This data is presented for reference. For a direct comparison see the energy density results below.

Analytic Averages

	U+U Tip-Tip	U+U Body-Body	Au+Au (b=0)
N_{part}	345	329	394
N_{coll}	1231	1102	1303

Clearly the results for the analytic simulation are suspect. According to these results N_{part} and N_{coll} are greater for central Au+Au collisions than either the tip to tip or body to body collision configurations of Uranium.

Monte-Carlo Averages

	U+U Tip-Tip	U+U Body-Body	Au+Au (b=0)
N_{part}	465 ± 4	461 ± 4	380 ± 4
N_{coll}	1748 ± 69	1351 ± 54	1183 ± 55

The results of the Monte-Carlo simulation, however, show that there is an increase in N_{part} and N_{coll} as we would expect. The data shows that there is less than a 1% increase in N_{part} between body to body collisions and tip to tip collisions of Uranium. The results for N_{coll} show that there is a 29% increase between body to body and tip to tip collisions of Uranium.

Distribution of Collision Parameters

The resulting distributions of the five collision parameters of U+U collisions can be seen in the plots in the appendix. In both the analytic and Monte-Carlo simulations the polar angle and impact parameter are distributed as one would expect – a distribution consistent with sampling phase space uniformly. In the analytic simulation cuts on the top 5% and 10% of N_{part} result in maximum impact parameters of about 5 and 5.25 fm respectively. [Figure A1, A2] Likewise, cuts on the top 5% and 10% of N_{part} in the Monte-Carlo simulation results in maximum impact parameters of about 4.25 and 6 fm. [Figure A3, A4]

The most interesting results of the distributions occur in the azimuth angle. In both of the simulations, and with both 5 and 10% cuts on N_{part} , the distributions of the azimuth angle exhibit bi-modal behavior. [Figure A3,A4] This is consistent with what was expected. The most numerous events in the 5% and 10% cuts on N_{part} are the events with azimuth angle near 0 (tip to tip), π (body to body), and 2π (tip to tip). [Figure A1-A4]

Performing a similar analysis on Au+Au collision yields the expected results. The polar angle and impact parameter are distributed as one would expect to sample phase space. In the Monte-Carlo simulation the maximum impact parameters for

the top 5% and 10% of N_{part} are about 4 and 5.5 fm respectively.

Importantly, the Monte-Carlo simulation shows there are no significant trends in the azimuth angle. This means the gold nuclei are invariant under rotations as they should be since they are modeled as spheres. [Figure A5, A6]

Energy Density

The charged multiplicity density per unit transverse area, $\frac{1}{S} \frac{dN_{ch}}{dy}$, is often associated with the energy density of nuclei collisions because particle production increases as it increases. Here S is the transverse area of the overlap zone weighted by the number of participating nucleons [2]

$$S = \pi \sqrt{\langle x^2 \rangle \langle y^2 \rangle}. \quad (5)$$

Where $\langle x^2 \rangle$ and $\langle y^2 \rangle$ are the averages of the squares of the x and y locations of the participant nucleons. The charged particle multiplicity per unit rapidity, $\frac{dN_{ch}}{dy}$, can be computed with the N_{part} and N_{coll} from the simulations, constants found to fit PHOBOS data, and the following parameterization

$$\frac{dN_{ch}}{dy} \cong 1.15 \frac{dN_{ch}}{d\eta}, \quad (6) [2,5]$$

$$\frac{dN_{ch}}{d\eta} = n_{pp} \left(x N_{coll} + (1-x) \frac{N_{part}}{2} \right). \quad (7) [2,6]$$

Where $n_{pp}=2.19$ and $x=.15$ at 200GeV. [2,12] Thus, the change in energy density from Au+Au collisions at b=0 to tip on tip U+U collisions can be inferred from the simulation data.

The analytic simulation resulted in a 15% increase in energy density for U+U tip to tip collisions when compared to central Au+Au collisions. A 17% decrease in energy density was observed in the analytic simulation of body to body U+U collisions when compared to central Au+Au collisions.

The Monte-Carlo simulation resulted in a 35% increase in energy density for tip to tip U+U collisions when compared to central Au+Au collisions. A 9% decrease in energy density was observed in the Monte-Carlo simulation for body to body U+U collisions when compared to central Au+Au collisions.

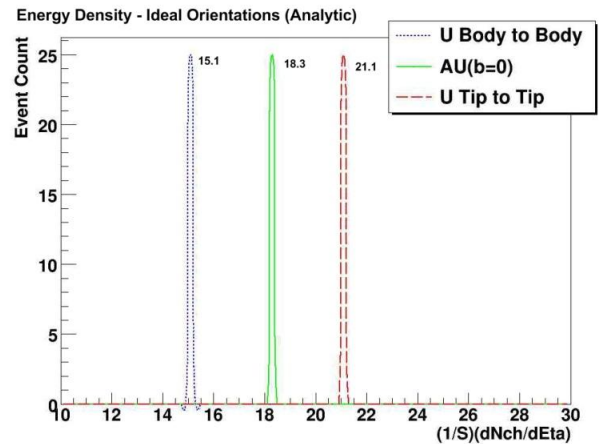


[Figure 4]

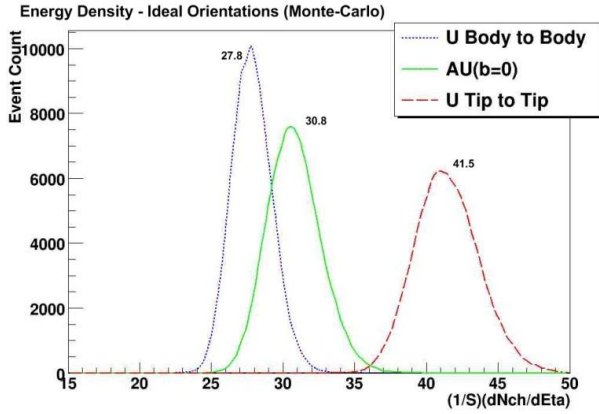


[Figure 5]

Although U+U collisions in the tip to tip configuration show a significant increase in energy density when compared to central Au+Au collisions there is no way to polarize the beam so that only tip to tip collisions occur. Instead collisions of all orientations occur. Events of importance must be selected by triggering methods such as cuts on particle multiplicity. Since the highest multiplicities occur at the highest $dN_{ch}/d\eta$ a cut is made on the top 5% of this quantity in an effort to observe an expected energy density distribution. This cut shows that there is neither a significant increase nor decrease in the mean observed energy density of U+U collisions when compared to Au+Au collisions. [Figures 6,7]

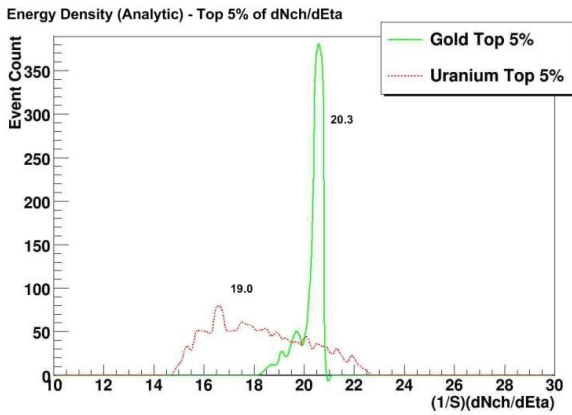


[Figure 6]

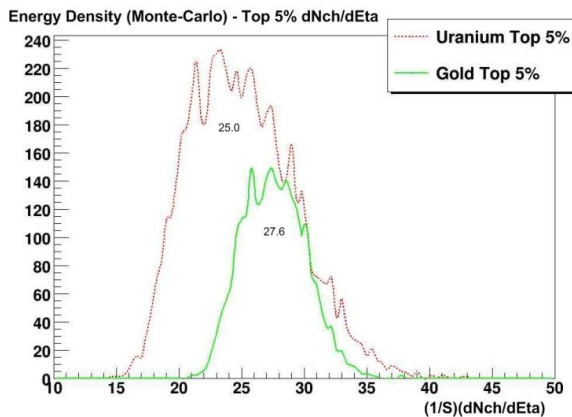


[Figure 7]

Upsilon Production

As noted before an increase in energy density also means an increase in particle production. This increase in particle production, in turn, increases the number of Upsilon produced per collision. This is because the expected Upsilon production from a U+U collision depends on the number of nucleon-nucleon collisions, N_{coll} . The number of produced Upsilon can be computed with the following where $\sigma_Y=82\text{pb}$ and $\sigma_{pp}=42\text{mb}$.

$$N_Y = \frac{\sigma_Y}{\sigma_{pp}} N_{coll} \cdot \quad (8)$$

N_{coll} is varied by scanning over possible impact parameters. For instance, the Upsilon production of the tip to tip configuration is tested by orienting the nuclei with $\theta_1=\theta_2=\phi_1=\phi_2=0$ and varying the impact parameter, b . Figures 8 and 9 show the results of this analysis for the analytic and Monte-Carlo simulations of U+U and Au+Au collisions. Here the phrase “nose to nose” is used synonymously with “tip to tip.”

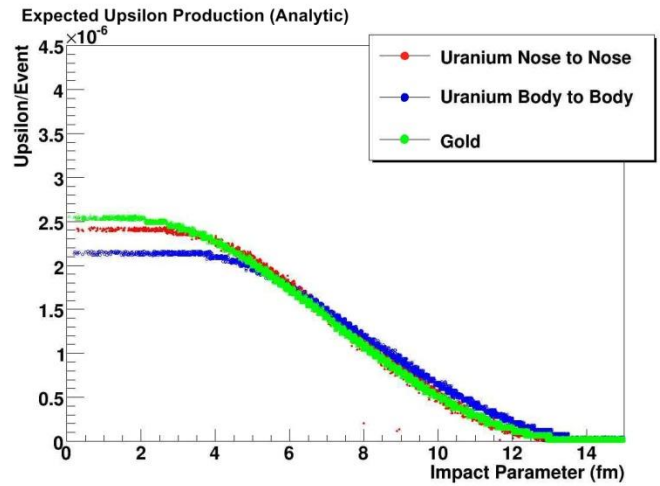


[Figure 8]

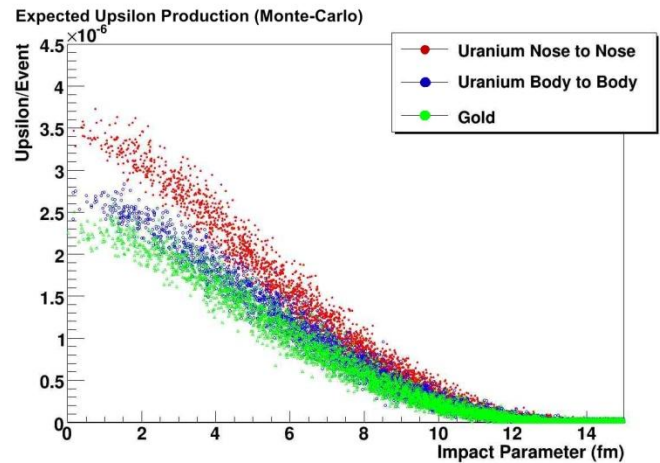


[Figure 9]

Clearly these results are not in agreement. The analytic simulation suggests that central Au+Au collisions will produce more Upsilon than either the tip to tip configuration or body to

body configurations of U+U collisions. Because the analytic simulation suffers from an as yet unidentified error they are disregarded and presented here only for completeness.

The Upsilon production results of the Monte-Carlo simulation show that collisions of Uranium in the tip to tip configuration will result in higher Upsilon production at any given impact parameter when compared with a Gold collision at the same impact parameter. Additionally, the results show that collisions of Uranium in the body to body configuration will result in a higher production of Upsilon when compared to Gold out to an impact parameter of approximately 8 fm.

IV. CONCLUSION

The Monte-Carlo simulation results of this study show several effects of the prolate spheroid geometry of the uranium nucleus. It was shown that the azimuth angle exhibits bi-modal behavior in the top 5% and 10% of N_{part} . [FigureA3, A4] The peaks of this distribution fall at $0, \pi$, and 2π , which is consistent with tip to tip, body to body, and tip to tip collisions respectively. Furthermore, the energy density analysis shows that energy density increases by 35% for tip to tip collisions of Uranium and decreases by 10% for body to body collisions when compared to central Gold collisions. However, when a cut is made on the top 5% of $dN/d\eta$ there is no appreciable difference in expected energy densities between U+U and Au+Au collisions. [Figure 6 ,7]

Furthermore, these results show that while U+U collisions do increase the energy density of collisions when in the tip to tip configuration there is no average increase in energy density when all the collision parameters are included. As a result, it can be concluded that given the same number of U+U collisions as Au+Au collisions no increase in the number of Upsilon produced will be observed.

V. FUTURE WORK

Work to correct the problematic results of the Analytic Simulations will continue throughout the fall 2009 semester. Additionally, improvements to the model will be discussed and implemented where necessary. Finally, cross checking with other independently found results will be performed to ensure the validity of these results.

VI. ACKNOWLEDGEMENTS

I would like to thank Daniel Cebra for his time, effort, and mentorship throughout the course of the summer. Without him and his active participation in project none of these results would be possible. I would also like to thank Jim Draper for his contributions to this project including developing an independent model for comparison and advising on and suggesting changes to the model presented here. His patience and knowledge has been indispensable. Additionally, I would like to thank Manuel Calderon his mentorship over the summer.

Finally, I would like to thank Rena Zieve for directing a fantastic REU program – one that I am incredibly appreciate for being a part of. This work was funded by the NSF.

-
- [1] U. Heinz and A. Kuhlman, Phys. Rev. Lett. 94, 132301 (2005).
 - [2] C. Nepali, G. Fai, D. Keane, Phys. Rev. C 73, 034911 (2006).
 - [3] F. K. McGowan, C. E. Bemis, Jr., J. L. C. Ford, Jr., W. T. Milner, R. L. Robinson, and P. H. Stelson, Phys. Rev. Lett. 27, 25, (1971).
 - [4] W. T. Milner, C. E. Bemis, Jr., and F. K. McGowan, Phys. Rev. C 16, 4, (1977).
 - [5] C. Adler *et al.* (STAR Collaboration), Phys. Rev. C 68, 034903 (2003).
 - [6] D. Kharzeev and M. Nardi, Phys. Lett. B507, 121 (2001)
 - [7] U. Heinz, Nucl. Phys. A 721, 30c (2003).
 - [8] M. Gyulassy, nucl-th/0403032.
 - [9] E. V. Shuryak, Nucl. Phys. A 750, 64 (2005).
 - [10] B. Muller, Nucl. Phys. A 721, 30c (2003).
 - [11] R. Vogt, *Ultrarelativistic Heavy-Ion Collisions* (2007)
 - [12] B. B. Back *et al.* (PHOBOS Collaboration), Phys. Rev. C 65, 061901 (R) (2002).
 - [13] Private Communications with Daniel Cebra, UC Davis
 - [14] Private Communications with Jim Draper, UC Davis

Appendix

Collision Distributions

Note: Blue corresponds to variable for nucleus 1; Red Corresponds to variable for Nucleus 2

Uranium Collision Orientation - Top 5% of N_{part} (Analytic)

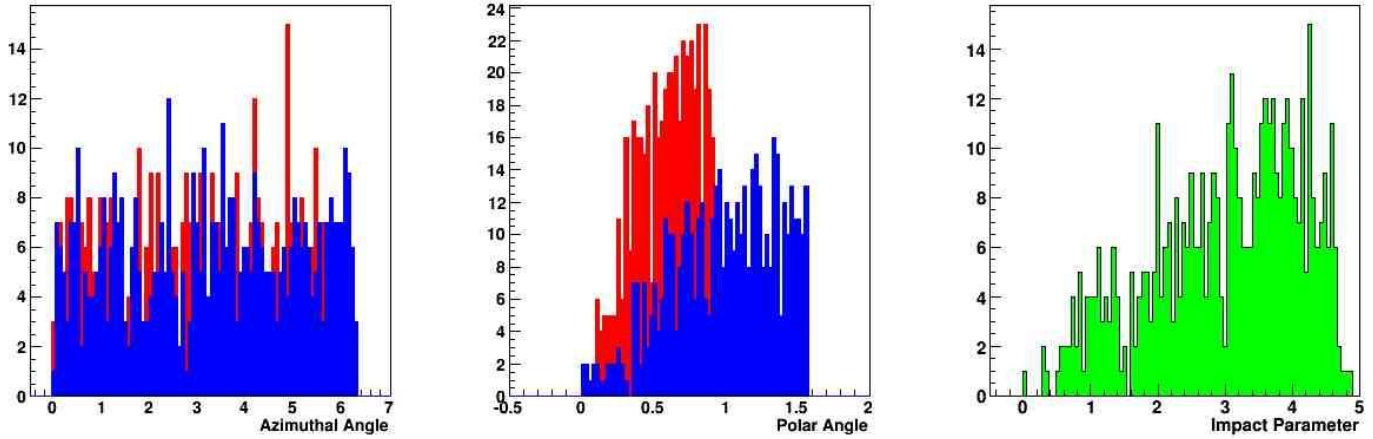


[Figure A1] Analytic Uranium Top 5% of N_{part}

Uranium Collision Orientation - Top 10% of N_{part} (Analytic)

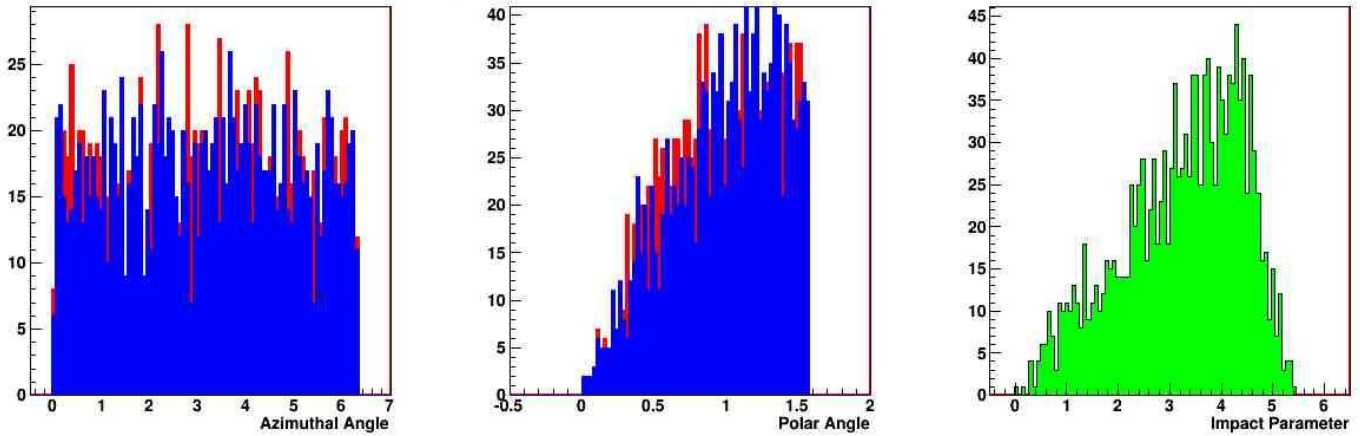


[Figure A2] Analytic Uranium Top 10% of N_{part}

Uranium Collision Orientation - Top 5% of N_{part} (Monte-Carlo)

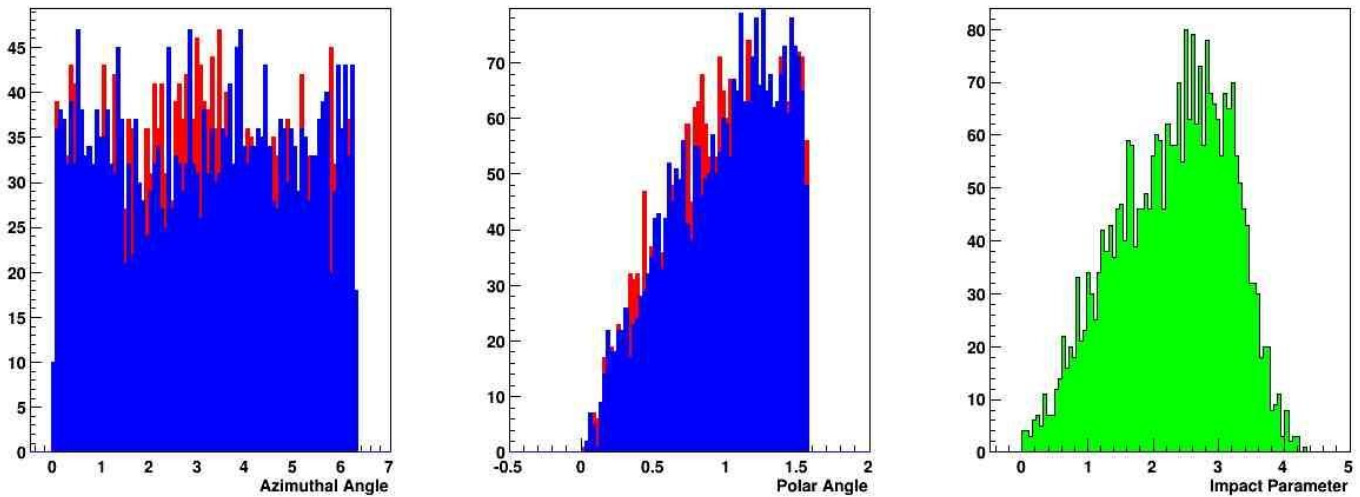


[Figure A3] Monte-Carlo Uranium Top 5% of N_{part}

Uranium Collision Orientation - Top 10% of Npart (Monte-Carlo)

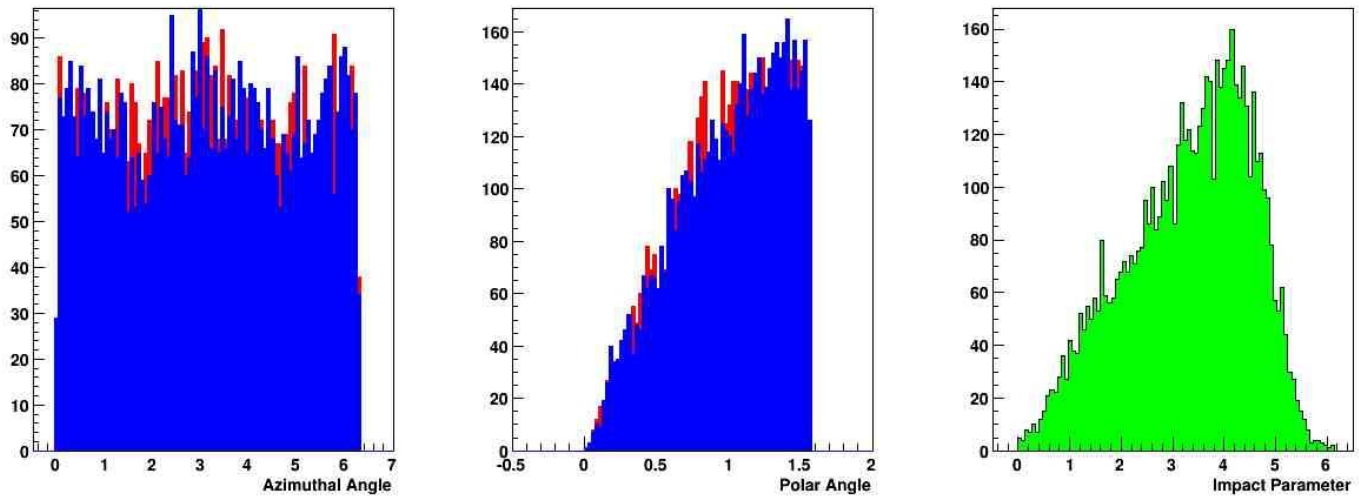


[Figure A4] Monte-Carlo Uranium Top 10% of N_{part}

Gold Collision Orientation - Top 5% of Npart (Monte-Carlo)

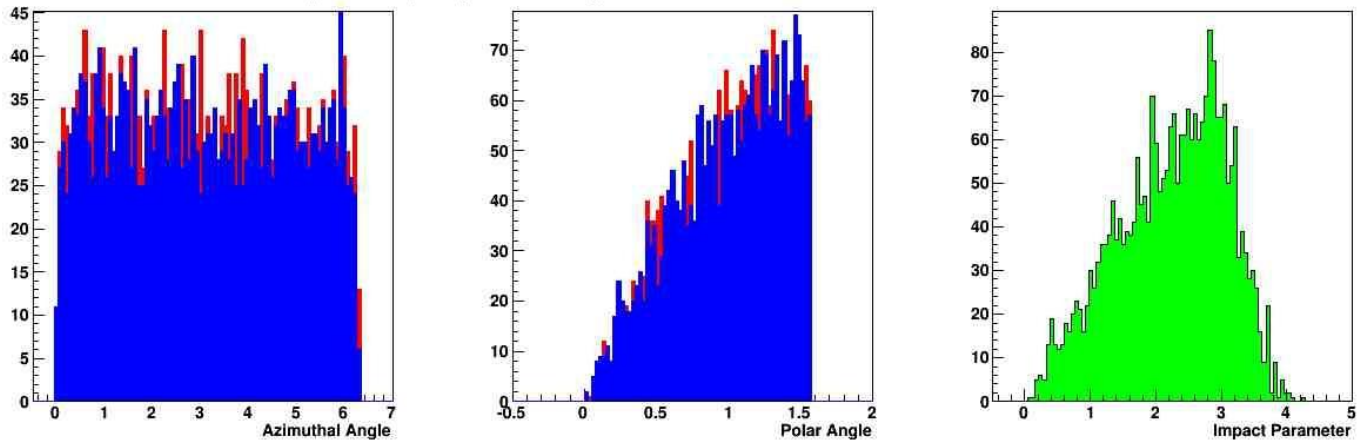


[Figure A5] Monte-Carlo Gold – Top 5% of N_{part}

Gold Collision Orientation - Top 10% of Npart (Monte-Carlo)

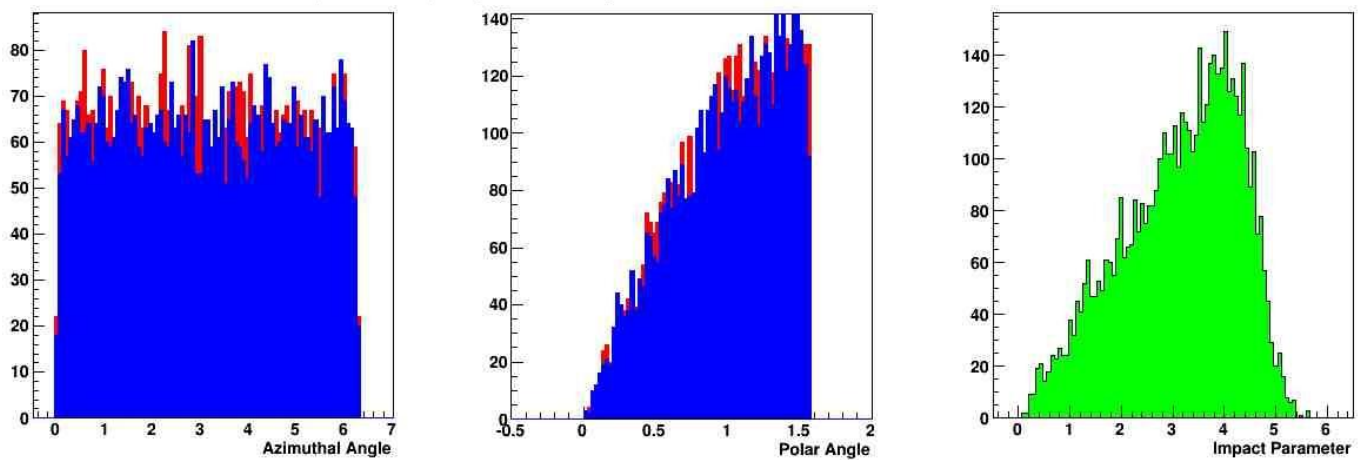


[Figure A6] Monte-Carlo Gold – Top 10% of N_{part}

Uranium and Gold Results

Note: Green is top 5% of variable; Green + Blue is top 10% of variable

Analytic Gold Results (Event Count vs. N)

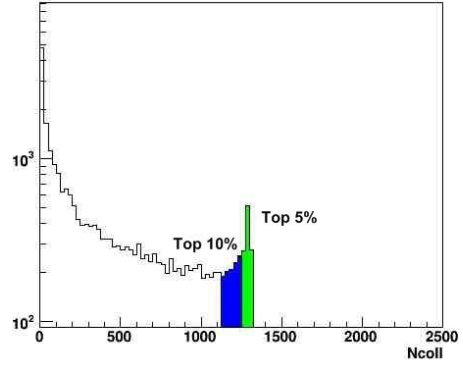
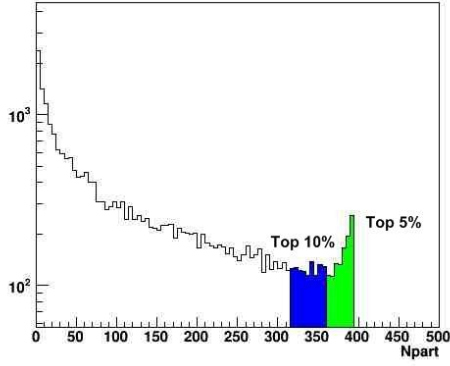


[Figure A7] Analytic Gold Result

Monte-Carlo Gold Results (Event Count vs. N)

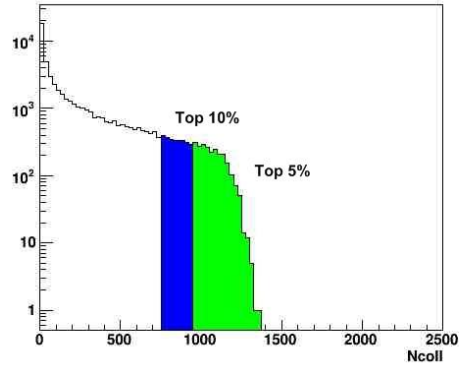
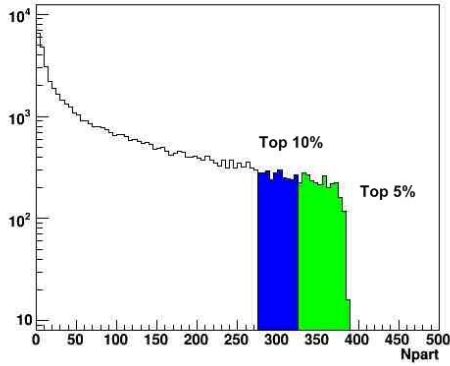


[Figure A8] Monte-Carlo Gold Results

Analytic Uranium Results (Event Count vs. N)

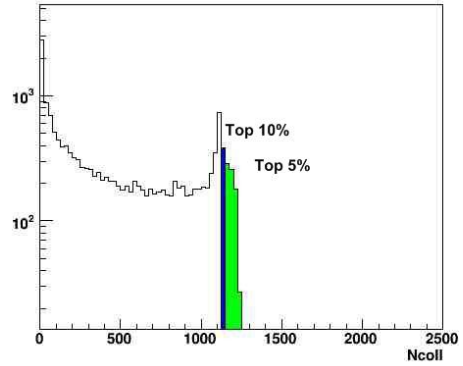
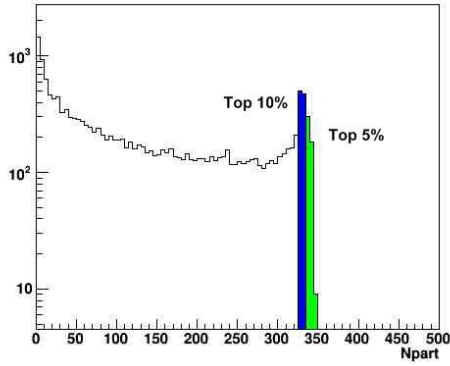


[Figure A9] Analytic Uranium Results

Monte-Carlo Uranium Results (Event Count vs. N)

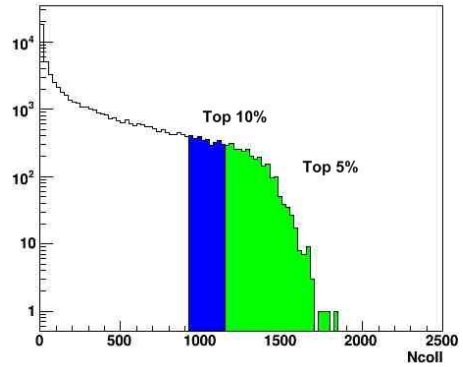
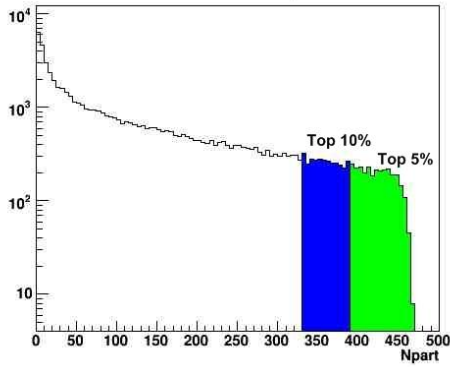


[Figure A10] Monte-Carlo Uranium Results